Liquid Chromatography/Mass Spectrometry Sequencing Approach for Highly Sulfated Heparin-derived Oligosaccharides*

Charuwan Thanawiroon‡, Kevin G. Rice‡, Toshihiko Toida§, and Robert J. Linhardt‡¶‖

From the ‡Division of Medicinal and Natural Products Chemistry, University of Iowa, Iowa City, Iowa 52242, the §Department of Bioanalytical Chemistry, Graduate School of Pharmaceutical Sciences, Chiba University, Chiba 263, Japan, and the ¶Departments of Chemistry, Biology, and Chemical and Biological Engineering, Rensselaer Polytechnic Institute, Troy, New York 12180

Liquid chromatography/mass spectrometry (LC/MS) is applied to the analysis of complex mixtures of oligosaccharides obtained through the controlled, heparinase-catalyzed depolymerization of heparin. Reversed-phase ion-pairing chromatography, utilizing a volatile mobile phase, results in the high resolution separation of highly sulfated, heparin-derived oligosaccharides. Simultaneous detection by UV absorbance and electrospray ionization-mass spectrometry (ESI-MS) provides important structural information on the oligosaccharide components of this mixture. Highly sensitive and easily interpretable spectra were obtained through post-column addition of tributylamine in acetonitrile. High resolution mass spectrometry afforded elemental composition of many known and previously unknown heparin-derived oligosaccharides. UV in combination with MS detection led to the identification of oligosaccharides arising from the original non-reducing end (NRE) of the heparin chain. The structural identification of these oligosaccharides provided sequence from a reading frame that begins at the non-reducing terminus of the heparin chain. Interestingly, 16 NRE oligosaccharides are observed, having both an even and an odd number of saccharide residues, most of which are not predicted based on biosynthesis or known pathways of heparin catabolism. Quantification of these NRE oligosaccharides afforded a number-averaged molecular weight consistent with that expected for the pharmaceutical heparin used in this analysis. Molecular ions could be assigned for oligosaccharides as large as a tetradecasaccharide, having a mass of 4625 Da and a net charge of −32. Furthermore, MS detection was demonstrated for oligosaccharides with up to 30 saccharide units having a mass of >10,000 Da and a net charge of −60.

The structural elucidation of complex carbohydrates remains one of the most difficult challenges for chemists, often requiring the application of multiple analytical approaches (1–5). Glycosaminoglycans (GAGs),[1] and heparin in particular, have

proven to be extremely difficult to analyze because of high negative charge, polydispersity, and sequence heterogeneity (6, 7). Heparin and low molecular weight heparins, prepared through the controlled chemical or enzymatic fragmentation of heparin (8), are widely used as clinical anticoagulants. Despite their medical importance, these drugs are relatively uncharacterized in terms of their chemical structure. Moreover, heparin and the structurally related heparan sulfate exhibit many additional biological activities, making them of great interest in new drug discovery (9). Numerous challenges can arise from the structural investigation of biologically active heparin oligosaccharides, particularly those in recognition systems involving specific protein-carbohydrate interactions (10, 11). Such biologically important oligosaccharides often contain rare sequences (12, 13) and are present only in minute, often picomole quantities. New derivatization methods (14, 15), chromatography (15, 16), electrophoresis-based separations (3), NMR (17, 18), and mass spectrometry (19–26) have been applied in the past to solve many of these complex structures. A successful combination of detection, separation, and spectral techniques might provide a critical advantage in understanding GAG structure.

NMR spectroscopy is an invaluable tool for the structural elucidation of GAGs, affording saccharide composition, ring conformation, glycosidic linkage, and sulfation patterns (17, 18, 27). Unfortunately, this technique is limited by the requirement of relatively large amounts (10 nmol to 1 μmol) of pure oligosaccharide sample. Mass spectrometry (MS) is another powerful technique for structural elucidation of GAGs. Soft ionization methods, including electrospray ionization (ESI) and matrix-assisted laser desorption/ionization (MALDI), have been amazingly successful in the analysis of neutral oligosaccharides and their peptide and lipid conjugates (28–31). The analysis of polyanionic GAG-oligosaccharides, such as those derived from heparin and heparan sulfate, is still in its infancy (28, 32).

MS studies have focused on the analysis of oligosaccharides prepared through the controlled enzymatic depolymerization of polysaccharides. MALDI time-of-flight (TOF) MS (19, 26) and ESI-MS (20, 23, 33, 34) have been the most favored approaches for the analysis of GAG-derived oligosaccharides. Both ESI-MS and MALDI-TOF-MS enjoy particular advantages in the analysis of large polar macromolecules. In MALDI, the major ion formed is typically the singly charged species, making MALDI-TOF-MS well suited to the analysis of mixtures. However, the

---

‖ To whom correspondence should be addressed. Tel.: 518-276-3404; Fax: 518-276-3405; E-mail: linhar@rpi.edu.

[1] The abbreviations used are: GAG, glycosaminoglycan; LC, liquid chromatography; MS, mass spectrometry; MALDI-TOF, matrix-assisted laser desorption/ionization time-of-flight; ESI-MS, electrospray ionization-MS; HPLC, high performance liquid chromatography; RPIP,

Reversed-phase ion-pairing; TrBA, tributylammonium acetate; dp, degree of polymerization; GlcA, glucuronic acid; IdoA, iduronic acid; GlcN, glucosamine; HexN, hexosamine; P, pyranose; S, sulfo; Ac, acetyl; NRE, non-reducing end.

This paper is available on line at http://www.jbc.org

ion yield depends on the chemical nature and size of the analyte, and MALDI is sufficiently energetic to damage the analyte. In contrast, ESI-MS utilizes a flowing stream containing the analyte, provides for very gentle ionization, and can be easily combined with on-line liquid-phase separation techniques, such as high performance liquid chromatography (HPLC) and capillary electrophoresis.

True molecular weight distributions of polysaccharides are difficult to measure by MS because of their polydispersity ($P = M_W/M_N > 1$). MALDI-TOF analysis of synthetic polymers, which are in many respects similar to polysaccharides (*e.g.* polydisperse, long-chain oligomers with distinct repeating units), cannot provide accurate molecular weight distributions of polymers with $P > 1.2$ (35, 36). Prior fractionation is required to simplify these polydisperse mixtures prior to MALDI-TOF (37, 38). On-line LC/ESI-MS eliminates time-consuming fraction collection, associated with such off-line MALDI-TOF analysis (24, 25). MALDI-TOF MS has also been used to determine the sequences of purified GAG-derived oligosaccharides through ion-pairing with a basic peptide and determining the mass of the peptide-oligosaccharide complex (26, 39). By combining controlled enzymatic or chemical depolymerization with MALDI-TOF-MS analysis of such complexes, it is possible to deduce oligosaccharide sequence (26, 39).

ESI-MS analysis of GAG-derived oligosaccharides is particularly promising due to the relative soft ionization technique that electrospray offers (20, 23, 25, 33, 40). On-line LC/MS also greatly enhances the analysis of complex mixtures of GAG-derived oligosaccharides. Strong anion exchange-HPLC conventionally used to fractionate GAG-derived oligosaccharide mixtures (16, 41) is difficult to interface with MS due to the high ionic strength mobile phases required to elute multiply charged oligosaccharides. Reversed-phase ion-pairing (RPIP)-HPLC, relying on tetraalkyl ammonium salts, provides excellent chromatographic resolution; however, these ion-pairing reagents are non-volatile and are required at high concentrations, making them incompatible with ESI-MS. Volatile ion-pairing reagents (42, 43), post-column removal of ion-pairing reagent with an in-line membrane (44), post-column addition of sheath liquid, and the splitting of the eluent flow (45) have all been used to overcome these problems. Recently, heparosan (an unsulfated, carboxyl-containing heparin analog) oligosaccharides have been successfully analyzed by RPIP-HPLC/ESI-MS (46). This method, however, has not been applied to large and highly sulfated oligosaccharides. The present study applies RPIP-HPLC/ESI-MS to the analysis of highly charged heparin-derived oligosaccharides to obtain both molecular weight and sequence information on the present heparin polymer.

EXPERIMENTAL PROCEDURES

Materials—Bovine lung heparin, sodium salt ($\geq$140 USP units/mg, 500,000 units) was from Sigma. Heparinase (heparin lyase I, EC 4.2.2.7) was from IBEX (Montreal, Canada). Acetonitrile, HPLC-grade, and all other chemicals, of the purest grade available, were obtained from Aldrich. Ultrapure water was obtained using a Milli-Q system (Millipore, Billerica, MA).

Preparation of Heparin Oligosaccharide Mixtures—The heparin oligosaccharide mixture was prepared from bovine lung heparin by controlled enzymatic depolymerization with heparinase as described previously (17). Briefly, 1 mg of heparin was digested with 0.2 milliunits of heparinase (EC 4.2.2.7) in 200 μl of 50 mM sodium phosphate buffer (pH 7.0) at 30 °C. The reaction mixture was incubated until the digestion was 30% complete, and then the mixture was boiled at 100 °C for 2 min to inactivate the enzyme. The mixture was freeze-dried and redissolved in 100 μl of double distilled water.

Chromatographic Conditions—HPLC separations were performed on a 5-μm Discovery C18 column (4.6 × 250 mm) from Supelco (Bellefonte, PA). Eluent A was water/acetonitrile (80:20), and eluent B was water/acetonitrile (35:65). Tributylamine (15 mM) and ammonium acetate (50 mM) were added to both eluents. The mobile phase pH was adjusted to

7.0 with acetic acid. The sample (20 μl, 10 mg/ml) was injected, and a linear gradient (from 0 to 100% eluent B in 120 min) at a flow rate of 0.5 ml/min was used for elution.

Off-line UV-LC measurements were performed using a Shimadzu HPLC system consisting of two Shimadzu LC-10A*i* pumps and a Shimadzu UV-visible spectrophotometric detector (Model SPD-10A). The elution profiles were monitored by absorbance at 232 nm at 0.02 absorbance units at full scale. On-line HPLC measurements were carried out on an Agilent 1100 series pumping system (Agilent Technologies, Inc.) consisting of a G1312A binary gradient pump, a G1322A vacuum degasser, a G1367A well plater sampler, and a GB65B multiple wavelength UV/VIS detector.

Mass Spectrometric Conditions—ESI mass spectra were obtained using an Agilent 1100 series Classic G2445A LC/MSD trap (Agilent Technologies, Inc.). Optimization was performed by direct injection (6 μl/min, 1 mg/ml) of trisulfated heparin disaccharide (Fig. 1, $n = 0$) with mobile phase A at a flow rate of 0.5 ml/min. The electrospray interface was set in negative ionization mode with the skimmer potential −19.7 V, capillary exit −48.4 V, and a source of temperature of 350 °C to obtain maximum abundance of the standard disaccharide ions in full scan spectra (200–2200 Da, 10 full scans/s). Nitrogen was used as a drying (12 liters/min) and nebulizing gas (60 p.s.i.). Total ion chromatograms and mass spectra were processed using Agilent Chemstation A.07. Software versions were as follows: 4.0 LC/MSD trap control 5.0 and Data Analysis 2.0 (Agilent Technologies, Inc.). Monoisotopic masses are reported throughout the text. For MS simplification experiments, the post-column addition reagents were (optimally 5 mM tributylammonium acetate (TrBA) in CH_3CN) directly infused into the ESI source using an Agilent syringe pump at flow rate of 6 μl/min. Both the sample and the post-column addition reagent were sprayed at the same time to ensure in-source mixing.

RESULTS AND DISCUSSION

Heparin (and heparan sulfate) are structurally diverse, high molecular weight (MWavg > 10,000), polydisperse ($P \approx 1.1$–1.4) mixtures (9, 47). Heparinase is used in reducing the molecular weight of this mixture to prepare low molecular weight heparins (8) and to facilitate the isolation and purification of specific heparin oligosaccharide components, through tedious and repetitive chromatography (10). Bovine lung heparin was selected as the starting material in this study as it has a reduced structural complexity, when compared with porcine intestinal heparin, because of its relatively high proportion of trisulfated disaccharide sequences of the structure →4) 2-*O*-sulfo-α-L-idopyranosuronic acid (1→4) 2-deoxy-2-sulfamido-6-*O*-sulfo-α-D-glucopyranose (1→ [→4) α-L-IdoAp2S (1→4) α-D-GlcNpS6S (1→] (10). Controlled, partial (30%), heparinase-catalyzed depolymerization yielded a mixture comprised primarily of oligosaccharides ranging from disaccharide (degree of polymerization (dp) 2) to oligosaccharides larger than tetradecasaccharide (dp14) as confirmed by size exclusion chromatography and gradient PAGE (17, 47) (data not shown). This oligosaccharide mixture is known to contain oligosaccharides having primarily an even number of saccharide residues. Furthermore, one oligosaccharide sequence predominates (Fig. 1), and disaccharides (dp2) through tetradecasaccharides (dp14) have been purified from this mixture and characterized by multidimensional NMR spectroscopy (17).

Extensive experiments were undertaken to optimize the HPLC separation of both small (dp2–dp6) and large (dp10–dp14) heparin-derived oligosaccharides (48). RPIP-HPLC used an MS-friendly mobile phase including: volatile ion-pairing reagents, tributylamine; volatile inorganic salt, ammonium acetate; and an organic modifier, acetonitrile. The choice of volatile ion-pairing reagent represents a compromise between low alkyl chain length affording high volatility, required for compatibility with on-line MS and longer alkyl chain length affording higher on-column retention of heparin-derived oligosaccharides associated with enhanced resolution (48). TrBA provided optimal retention with MS compatibility. Organic cosolvent, solvent pH, temperature, gradient profiles of volatile inorganic

FIG. 1. **Structures of major heparin oligosaccharides derived from heparinase treatment of bovine lung heparin.** The net charge and molecular weight for the disaccharide (dp2, $n = 0$) are -4 and 577.5 (as the protonated form, M), and for the tetradecasaccharide (dp14, $n = 6$), they are -28 and 4042.4.
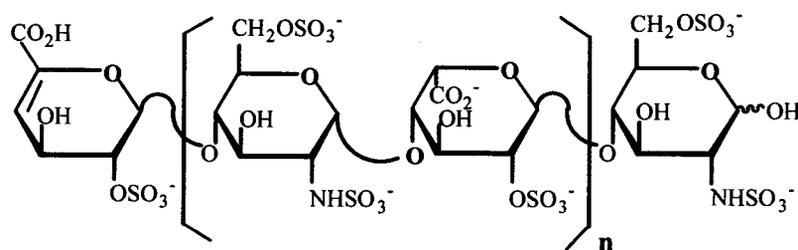
salt, and various ion-pairing reagents were first optimized, in off-line RPIP-HPLC using UV detection, to obtain efficient oligosaccharide separation (48). Ammonium formate and ammonium acetate gradients gave low peak intensities and complicated spectra due to ion suppression. RPIP-HPLC utilizing an acetonitrile gradient at a fixed concentration of ammonium acetate (50 mM), pH 7.0, and TrBA (15 mM) afforded both high chromatographic resolution and excellent MS analyses (Fig. 2).

In the mass spectral analysis of highly sulfated oligosaccharides, the partial ion-pairing of sulfo groups with various cations (*i.e.* sodium, potassium, ammonium, or ion-pairing reagent) can pose significant problems in ESI-MS analysis, affording a large number of pseudomolecular ions having different m/z values, resulting in highly complex spectra and decreased sensitivity (20, 33). The removal of cations has been successfully applied to the ESI-MS analysis of the DNA polyanion, affording spectra with predominantly singly charged ions closely resembling the simpler spectra obtained using MALDI-MS (49–53). In DNA analysis, post-column addition of organic solvent, ion-pairing reagent, and organic acids and organic bases, as a sheath liquid directly within the ion source, decreases the surface tension and increases the volatility of the electrosprayed solution, simplifying the mass spectra (49–53).

In the analysis of heparin-derived oligosaccharides, we also expected to observe a reduction in charge states from added acids (formic acid, acetic acid) and bases (ammonium hydroxide, piperidine, and imidazole) by influencing the proton transfer reactions, simplifying spectral complexity, and enhancing peak intensity. The addition of CH$_3$CN as sheath liquid resulted in improvement in ion intensity and the substantial spectral simplification, possibly by weakening of the solvent-solute and ion-counter-ion interactions and the subsequent release of free analyte ions to the evaporation process. The most intense ion peaks of each oligosaccharide caused by cation adduction are always associated with the TrBA adduct. The post-column addition of a low concentration (5 mM) of TrBA ion-pairing reagent in acetonitrile provided the most simplified spectra, suppressing the Na$^+$/NH$_4^+$ adduction without influencing the charge state reduction; however, a substantial reduction (5-fold) in ion intensity was observed.

Mass spectra, greatly simplified through post-column addition of 5 mM TrBA in CH$_3$CN, are shown in Fig. 3. Only one major peak is observed for the major di-, tetra-, hexasaccharide corresponding to the protonated forms. Two prominent peaks are observed for the major octa- through tetradecasaccharide corresponding to the TrBA adduct forms. Thus, a major advantage of post-column addition of TrBA/CH$_3$CN is the disappearance of other cation adduct peaks, resulting in a substantial reduction in "chemical noise," affording simplified and interpretable spectra. The optimized ESI mass spectra were successfully simplified, showing the elimination of cationic adducts for small oligosaccharides (dp2–dp6) and a decreased relative abundance of sodiated and ammoniated adducts for larger oligosaccharides (dp8–dp14) (Fig. 3). These optimized spectra were interpreted, and representative m/z values for all spectra are shown in Table I.

Spectra in the Fig. 3 were obtained for fully sulfated oligosaccharides (three sulfo groups/disaccharide unit) as indicated in the structure shown in Fig. 1. The negative ion ESI mass spectra of the small oligosaccharides (dp2–dp6) are easily interpreted. The molecular mass and the total number of sulfo groups can be determined from a series of molecular ions corresponding to m/z 576, $[M - xH]^{x-}$. ESI-MS shows a singly charged parent ion m/z 575.9, $[M - H]^-$ (M = 577 Da), for disaccharide (dp2), whereas the m/z 576.1 corresponded to doubly charged parent ion $[M - 2H]^{2-}$ (M = 1155 Da), for tetrasaccharide (dp4) and to a triply charged parent ion $[M - 3H]^{3-}$ (M = 1732.4 Da), for hexasaccharide (dp6) (Table I). The charge on these molecular ions can be determined from the mass differences of their isotopic ions, determined by high resolution scans using the ion-trap analyzer. This approach can distinguish isotopes of ions with up to five charges (*i.e.* differences as low as $\Delta m/z = 0.2$). The ^{13}C isotope of ion peaks for disaccharide, tetrasaccharide, and hexasaccharide were 0.9, 0.5, and 0.3 m/z units (Fig. 3), confirming that the ions were singly, doubly, and triply charged, respectively, as assigned in Table I. Isomeric disaccharides having three sulfo groups are isobaric and indistinguishable by ESI-MS. High resolution of RPIP-HPLC, however, is capable of separating positional isomers of isobaric oligosaccharides, of size dp $\leq$ 8, having identical charge and mass. Fig. 2 shows multiple, chromatographically resolved, fully sulfated, isobaric disaccharides through octasaccharides. The first and major member of each isobaric group corresponds to the structures ($n = 0–3$) shown in Fig. 1 as confirmed through co-injection of authentic standards (17). In the case of isomeric unsaturated trisulfated disaccharides **16**, **17**, and **18**, for example, structures containing ΔUAp2S and GlcNpS6S or GlcNpS3S or GlcNp3S6S or ΔUAp and GlcNpS3S6S would afford the correct mass, but all except this first disaccharide ΔUAp2SGlcNS6S **16** are infrequently encountered in heparin.

The negative ion ESI mass spectra of larger oligosaccharides (dp8–dp14) provide the mass from which the number of saccharide units, acetyl, and sulfo groups in each molecule can be deduced. A series of peaks are observed associated with adducts of the molecular ion with the ion-pairing reagent, TrBA. These peaks often have multiple negative charges and take the form $[M - (x + y) H + yTrBA]^{x-}$, where x = the number of protons and y = the number of TrBA$^+$ counter ions. The major peak corresponding to the fully sulfated octasaccharide (dp8) (Fig. 1) eluting at 39 min (Fig. 2), for example, gives a spectrum with two intense peaks at m/z 830.5 and m/z 892.0, assignable to $[M - 4H + TrBA]^{3-}$ and $[M - 5H + 2TrBA]^{3-}$, respectively (Fig. 3). These molecular ions both correspond to an octasaccharide substituted with 12 sulfo groups. Similarly, the major, fully sulfated, decasaccharide (dp10) (Fig. 1) shows a prominent peak at m/z 766.7, corresponding to $[M - 5H + TrBA]^{4-}$ (Fig. 3). The negative ion ESI mass spectra of higher oligosaccharides (dp12 and dp14) are similar but give ions with a higher negative charge. These data demonstrate that an increased number of saccharide units and sulfo groups results in
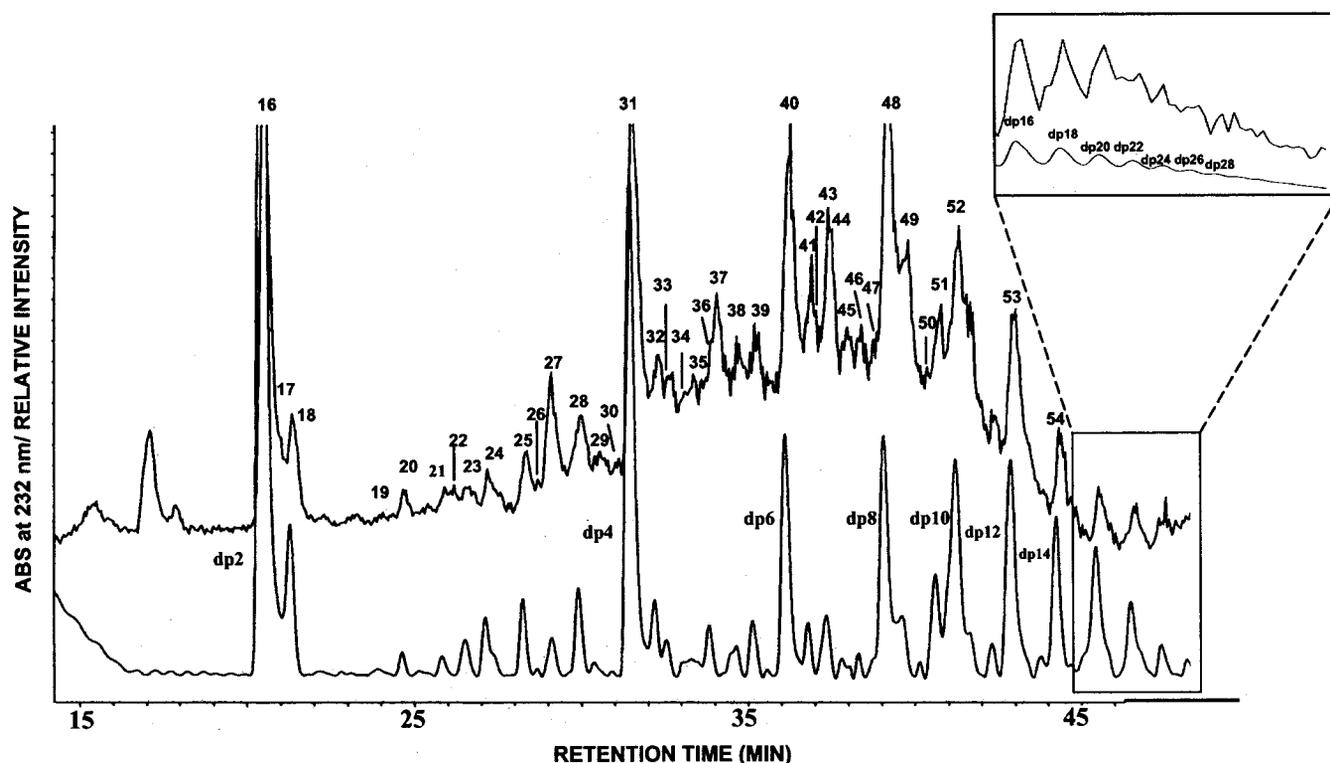
FIG. 2. **RPIP-HPLC separation of heparin oligosaccharides obtained from controlled (30%) heparinase depolymerization of bovine lung heparin.** A total ion chromatogram using negative ESI-MS detection (*upper trace*) with peaks numbered and a UV chromatogram at 232 nm (lower trace) with dp of peaks corresponding to the oligosaccharides in Fig. 1 are shown. The *inset* shows the expanded view of both the total ion chromatogram and the UV chromatograms of higher oligosaccharides assigned to dp16–dp28 by peak counting. Assignments for labeled peaks, based on ESI-MS spectra, are given in Table I.

stronger cation adduction and higher negative charge (Table I). The identity (Fig. 1, $n = 3-6$) of fully sulfated oligosaccharides (dp8–dp14) was confirmed through co-injection of authentic standards (17). Oligosaccharides of dp > 14 show prominent peaks corresponding to multiple $TrBA^+/NH_4^+/Na^+$ adducts, making interpretation of their spectra difficult.

The applicability of this method to analyze minor oligosaccharides that are not fully sulfated (<3 sulfo groups/disaccharide unit) was next examined by selecting minor peaks located between the major, fully sulfated, oligosaccharide peaks, labeled as dp2–dp14 (Fig. 2). The calculated molecular weight based on monoisotopic mass and observed m/z values for the prominent peaks associated with these undersulfated oligosaccharides are provided in Table I. A shallow acetonitrile gradient of half the slope was used to optimize the separation of undersulfated species eluting early prior to the fully sulfated disaccharide, dp2 (Fig. 4). The negative ion ESI mass spectra of these species was easily interpreted, giving a single protonated parent ion $[M - H]^-$ free of cationic adducts and permitting the determination of the number of saccharide units, sulfo groups, and acetyl groups (Fig. 4).

The heparinase (heparin lyase I) used in this study, to prepare oligosaccharides, was purified from *Flavobacterium heparinum*. This enzyme acts on heparin through a random, endolytic, β-eliminative mechanism (54) in which the glycosidic bond between an *N*-sulfo-6-*O*-sulfo (or OH) glucosamine residue to a 2-*O*-sulfo iduronic acid residue is cleaved, forming a C4–C5 unsaturated uronate residue at the non-reducing end of the product, conferring a chromophore that absorbs at 232 nm. Based on the average molecular weight (13,000) of the heparin starting material and the 30% completion of the heparinase-catalyzed depolymerization reaction, it was possible to calculate the mole percentage of products arising from the original non-reducing ends (NREs) of heparin chains as 10–12% (55).

These original NREs correspond to termination sequences in heparin biosynthesis and catabolism through the action of mammalian tissue heparanases and/or lysomal enzymes. The products derived from the non-reducing end of heparin should contain a uronic acid residue without a C4–C5 site of unsaturation, having a mass 18 atomic mass units greater than corresponding unsaturated product and with no absorbance at 232 nm. A detailed analysis of Fig. 2 shows 16 such saturated oligosaccharides, ranging in size from monosaccharide through decasaccharide. The structural diversity and molar ratio of the NRE oligosaccharides observed are difficult to rationalize on the basis of the known pathways for heparin biosynthesis and catabolism. The three saturated trisulfated disaccharides, **13**, **14**, and **15**, for example, could be comprised of IdoAp2S or GlcAp2S and GlcNpS6S or GlcNpS3S or GlcNp3S6S or GlcAp or IdoAp and GlcNpS3S6S, but all except this first disaccharide IdoAp2SGlcNS6S (presumably **13**) should be extremely rare in heparin. Two chains, one terminating at the NRE with a uronic acid residue and one with a glucosamine residue, can be used to demonstrate the principle of MS-based sequencing (Fig. 5). Computer simulation studies (56, 57) together with an improved understanding of the specificity of heparinase will be required to determine the precise number of possible non-reducing end terminal sequences present in bovine lung heparin. The saturated oligosaccharides observed correspond to 11.45% of the total oligosaccharides of dp ≤ 10, identical to the mathematically predicted value of 10–12% (55) and consistent with the known molecular weight of bovine lung heparin. Closure of mass balance suggests that virtually all the NRE oligosaccharides present have been identified.

The diverse and relatively abundant population of oligosaccharides terminated with saturated uronic acid residues, found in the current study, is somewhat surprising as others (58) have failed to observe saturated products. Moreover, it is pre-
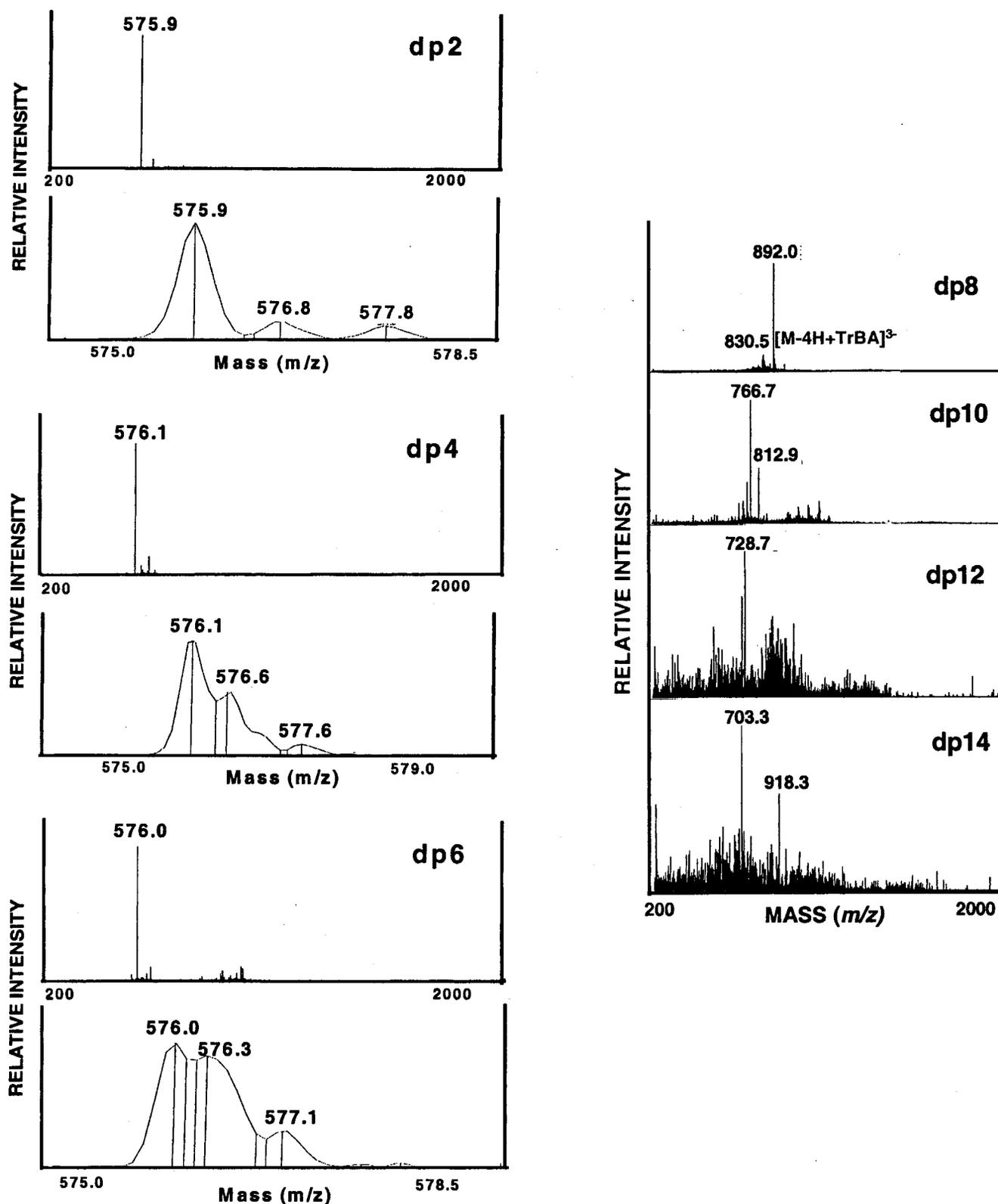
FIG. 3. **Electrospray ionization mass spectra of the fully sulfated heparin oligosaccharides ranging in size from disaccharide (*dp2*) to tetradecasaccharide (*dp14*).** The full scan spectra (*upper panel*) and narrow range spectra showing isotope distribution (*lower panel*) are presented for the oligosaccharides of dp2–dp6.

sumed that the bovine lung heparin starting material used in this study is formed through the action of heparanase on macromolecular heparin. Such products should be rare since this enzyme, an endo-glucuronidase, should generate only chains terminated at the non-reducing end with a glucosamine residue (59, 60). The presence and identity of these unusual products

containing saturated uronic acid is clearly supported by three experimental observations: (1) their slightly shorter retention time on RPIP-HPLC when compared with each of their unsaturated counterparts; (2) the absence of absorbance at 232 nm in HPLC, although a high ion-current is present in MS; and (3) their distinctive mass. The HPLC data clearly show the pres-

TABLE I
Major molecular ions in the ESI mass spectra of heparin-derived oligosaccharides and deduced compositions

Oligosaccharide size	Oligosaccharide composition[a]	Major ions observed	Oligosaccharide calculated	Mass theorized	Peak number
				Da	
Monosaccharide	HexNAcS	300.3 [M − H]−	301.3	301.047	2
Disaccharides	3S	575.9 [M − H]−	576.9	576.971	16, 17, 18
	* 3S, 1H$_2$O [b]	594.3 [M − H]−	595.3	594.982	13, 14, 15
	2S	496.4 [M − H]−	497.4	497.015	8, 10
	* 2S, 1H$_2$O	514.1 [M − H]−	515.1	515.025	6, 7
	1S	418.0 [M − H]−	419.0	417.058	12
	1S, 1Ac	458.4 [M − H]−	459.4	459.068	3, 4, 9
	0S	338.0 [M − H]−	339.0	337.101	5
	0S, 1Ac	378.5 [M − H]−	379.5	379.111	1
	* 0S,1Ac,1H$_2$O	397.9 [M − H]−	398.9	397.122	11
Trisaccharide	see Figure 5	840.9 [M − H]−	841.9	839.064	20
Tetrasaccharides	6S	576.1 [M − 2H]2−	1154.2	1153.943	31, 32
	* 6S, 1H$_2$O	585.8 [M − 2H]2−	1173.6	1171.953	27
	5S	536.4 [M − 2H]2−	1074.8	1073.986	25, 26, 28, 29
	* 5S, 1H$_2$O	545.0 [M − 2H]2−	1092.0	1091.996	21, 22
	4S	496.0 [M − 2H]2−	994.0	994.029	19
	* 4S,1Ac,1H$_2$O	527.5 [M − 2H]2−	1057.0	1054.050	30
	2S	415.7 [M − 2H]2−	833.4	834.115	23, 24
Pentasaccharide	see Figure 5	668.7 [M − 2H]2−	1339.4	1336.079	33
Hexasaccharides	9S	576.0 [M − 3H]3−	1731.0	1730.914	40, 41
	* 9S, 1H$_2$O	582.5 [M − 3H]3−	1750.5	1748.925	37
	8S	550.2 [M − 3H]3−	1653.6	1650.957	
		916.9 [M − 3H+TBA]2−	1651.4	1650.957	36, 38, 39
	6S, 2Ac	787.4 [M − 2H]2−	1576.8	1575.065	34
	4S, 2Ac	708.4 [M − 2H]2−	1418.8	1415.151	35
Octasaccharides	12S	892.0 [M − 5H + 2TrBA]3−	2310.3	2307.885	
		830.5 [M − 4H + TrBA]3−	2310.1	2307.885	48, 49
	* 12S, 1H$_2$O	898.2 [M − 5H + 2TrBA]3−	2328.9	2325.896	43
	11S	803.2 [M − 4H + TrBA]3−	2228.2	2227.929	
		865.4 [M − 5H + 2TrBA]3−	2230.5	2227.929	44, 45, 46
	10S	776.6 [M − 4H + TrBA]3−	2148.4	2147.972	42
	* 8S, 1H$_2$O	791.0 [M − 5H + 2TrBA]3−	2007.3	2006.457	47
Decasaccharides	15S	766.7 [M − 5H + TrBA]4−	2886.4	2884.857	
		812.9 [M − 6H + 2TrBA]4−	2886.9	2884.857	52
	* 15S, 1H$_2$O	771.0 [M − 5H + TrBA]4−	2903.6	2902.867	50
	14S	746.8 [M − 5H + TrBA]4−	2806.8	2804.900	51
Dodecasaccharide	18S	728.7 [M − 6H + TrBA]5−	3464.1	3461.828	53
Tetradecasaccharide	21S	703.3 [M − 7H + TrBA]6−	4041.4	4038.799	
		918.3 [M − 8H + 3TrBA]5−	4043.4	4038.799	54

[a] Oligosaccharide composition is based on the structure in Fig. 1. Ac corresponds to the number of acetyl groups, S corresponds to sulfo groups. H$_2$O is shown for oligosaccharides having an even number of saccharide units and arising from the non-reducing end of heparin.

[b] Oligosaccharides arising from the non-reducing end of the parent heparin are designated with an asterisk.
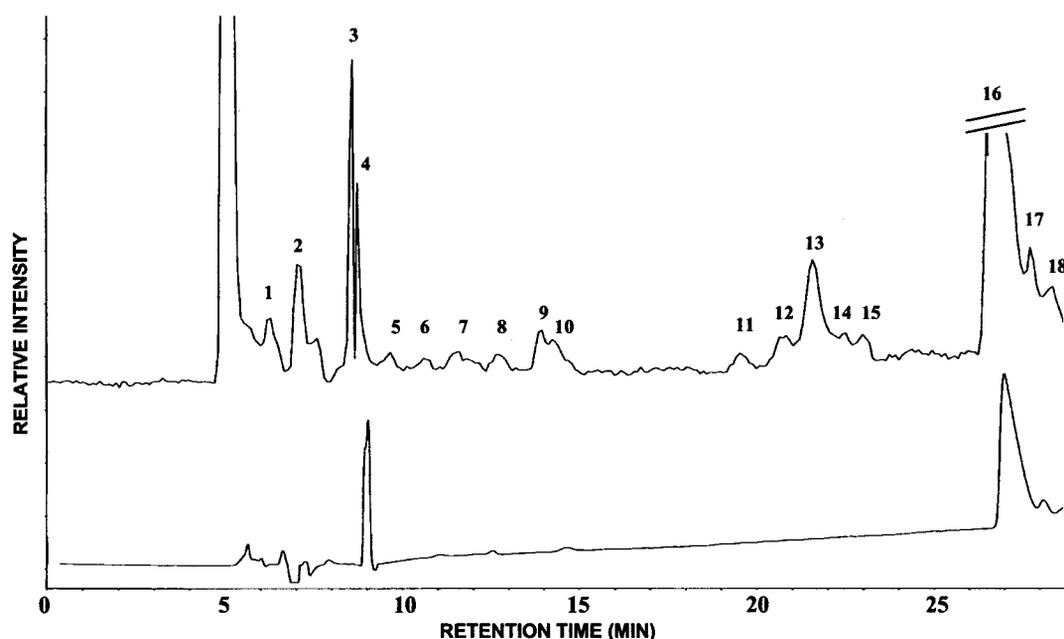

FIG. 4. **RPIP-HPLC separation of oligosaccharides eluted using a shallow acetonitrile gradient.** Peaks are labeled in the total ion chromatogram using negative ESI-MS detection (*upper trace*). The UV chromatogram at 232 nm (*lower trace*) shows the few peaks corresponding to products containing unsaturated uronic acid residues. Assignments for labeled peaks, based on ESI-MS spectra, are given in Table I. The spectra for the fully sulfated disaccharide (peak 16 corresponds to dp2; illustrated on Fig. 1, *n* = 0) are shown in Fig. 3.
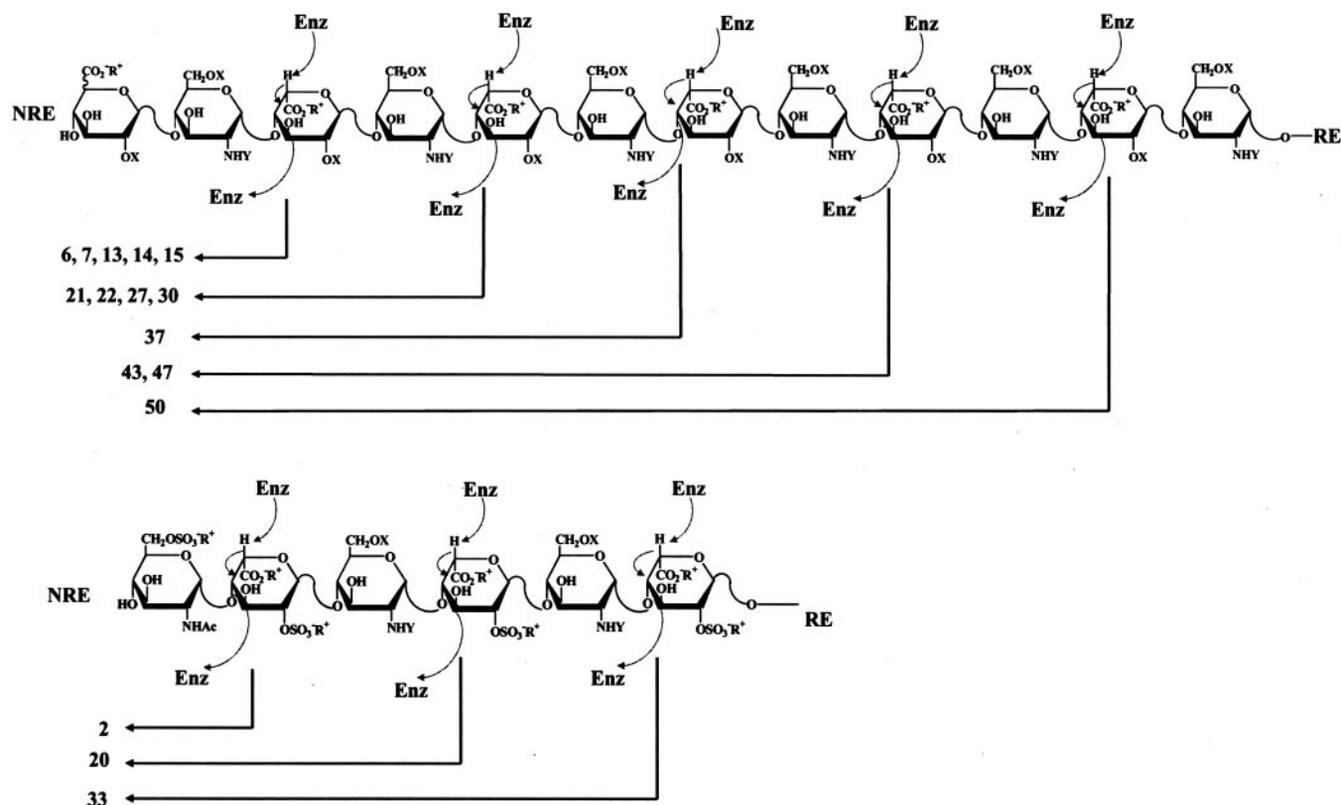
FIG. 5. **LC/MS sequencing of bovine lung heparin from the NRE.** For the upper structure (terminating in uronic acid), saturated disaccharide: 13, 14, 15 ($X = Y = SO_3^-R^+$), 6, 7 ($1X = SO_3^-R^+$, $1X = H$, $Y = SO_3^-R^+$); saturated tetrasaccharide: 27 ($X = Y = SO_3^-R^+$), 21, 22 ($3X = SO_3^-R^+$, $1X = H$, $Y = SO_3^-R^+$), 30 ($3X = SO_3^-R^+$, $1X = H$, $1Y = SO_3^-R^+$, $1Y = Ac$); saturated hexasaccharide: 37 ($X = Y = SO_3^-R^+$); saturated octasaccharide: 43 ($X = Y = SO_3^-R^+$), 47 ($4X = SO_3^-R^+$, $4X = H$, $Y = SO_3^-R^+$); saturated decasaccharide: 50 ($X = Y = SO_3^-R^+$). For the lower structure (terminating in glucosamine), saturated trisaccharide: 20 ($X = SO_3^-R^+$, $Y = Ac$); saturated pentasaccharide: 33 ($1X = SO_3^-R^+$, $1X = SO_3^-R^+$ or H, $1Y = Ac$, $1Y = SO_3^-R^+$ or H). The non-reducing end GlcNAc is unexpectedly observed as the monosaccharide, suggesting, but not confirming, that it is also at the non-reducing end of the trisaccharide **20** and pentasaccharide **23** products.

ence of unsaturated products prior to mass spectral analysis, ruling out the possibility that these products are simply a water adduct formed in the spectrometer.

The most prominent oligosaccharides, derived from bovine lung heparin, are comprised of the repeating unit →4) α-L-IdoAp2S (1→4) α-D-GlcNpS6S (1→. RPIP-HPLC easily separates oligosaccharides ranging from dp2–dp20, and ESI-MS affords a total ion chromatogram that closely parallels this chromatogram. The structures of the major oligosaccharides in each size class (Fig. 2, *dp2–dp14*) correspond to ΔUAp2S (1→ [4)-α-D-GlcNpS6S (1→4)-α-L-IdoAp2S (1]$_n$→4)-α-D-GlcNpS6S (where $n = 0$–6 and ΔUA is 4-deoxy-α-L-*threo*-hexenopyranosyl-uronic acid) (Fig. 1) as confirmed through the LC/MS of previously characterized oligosaccharide standards (17). The resolution of discrete portions of the chromatogram that are of particular interest can be improved by adjusting the acetonitrile gradient. For example, using a shallow gradient (Fig. 4), 1 monosaccharide peak and 17 disaccharide peaks including three clusters of peaks corresponding to isomeric oligosaccharides having identical molecular mass were determined. It is interesting to note that the only monosaccharide observed had an *m/z* 300 corresponding to HexNAcS, presumably GlcNAc6S (Fig. 5). This is certainly unexpected, as GlcNAc is rare in bovine lung heparin (61), which is instead rich in GlcNS. Moreover, the monosaccharide product reported previously from heparinase treatment of heparin had the structure GlcNS6S (58). We also fail to observe a trisaccharide product of the same mass as one having a non-reducing end GlcNS residue prepared previously from heparinase treatment of heparin (62). GlcNS, GlcNS6S, GlcNS3S, and GlcNS3S6S residues at the non-reducing end of heparin chains, expected based on the

specificity of human heparanase (59, 60), are surprisingly missing based on the absence of ions at *m/z* 228, 308, and 388. This suggests two possibilities: first, that bovine heparanase has a different specificity than human heparanase, or second, that other catabolic enzymes in bovine tissues are responsible for the absence of chains terminated with GlcNS residues and the presence of substantial quantities of products terminated with saturated uronic acid residues. Further studies on proteoglycans and glycosaminoglycan catabolism are warranted based on the results of the current analyses.

Despite the high resolution obtained, it is likely that certain peaks, particularly ones of higher dp, may contain multiple oligosaccharide components. The mass spectra of such peaks can be used to assign the mass of these individual components as long as they are not isobaric. Mass spectral data alone can be used to determine the dp of oligosaccharides having an identical *m/z* as long as a prominent ion of net charge of < -5 can be detected. As shown in Table I, such ions are found for oligosaccharides of size ranging from dp2 to dp10. At dp > 10, oligosaccharide size can be determined through the use of defined oligosaccharide standards (dp12–dp14) or peak counting in the RPIP chromatogram (dp>14).

Bovine lung heparin-derived oligosaccharides are among the most highly sulfated GAG-derived oligosaccharides, and their analysis clearly demonstrates the potential of LC/MS. Heparosan, an *Escherichia coli*-derived, unsulfated polysaccharide of the structure →4) β-D-GlcAp (1→4) α-D-GlcNpAc (1→, has been successfully analyzed previously by LC/MS following its treatment with heparintinase (heparin lyase III) (46). Using a shallow acetonitrile gradient molecular ion, information could be successfully obtained on heparosan-derived oligosaccharides as

large as dp32 (molecular weight = 6069.14), demonstrating the utility of this method for unsulfated polyanionic polysaccharides (data not shown). Other potential applications of the present method might include the analysis of structurally related GAGs including heparan sulfate, dermatan sulfate, chondroitin sulfate, and keratan sulfate. Of particular importance is developing a method for sequencing heparan sulfate. Heparan sulfate (0–1 sulfo groups/disaccharide) is more highly sulfated than heparosan (0 sulfo groups/disaccharide) but considerably less sulfated than bovine lung heparin (2.5–3 sulfo groups/disaccharide) (9). Most importantly, heparan sulfate is more structurally complex than heparin and is the endogenous molecule responsible for many physiological and pathophysiological activities commonly associated with heparin (10, 11). Substantial effort has been applied to the sequencing of heparan sulfate (63, 64) as well as heparin (14, 65–67). The detection of saturated oligosaccharides derived from the original non-reducing end of heparin chains in the current study suggests that it might be possible to obtain sequence information of heparan sulfate using the non-reducing end as a reading frame. Hascall and co-workers (68) have applied non-spectral methods to identify the NREs of chondroitin sulfate chains. Future studies will apply LC/MS to the sequencing of heparin, heparan sulfate, and other GAGs. Preliminary experiments using the MS/MS capabilities of the ion-trap instrument afforded fragmentation leading to the loss of sulfo groups. Additional MS/MS studies looking at a wide variety of experimental conditions will be necessary to obtain through-glycosidic and through-ring fragmentations and to determine the positioning of sulfo groups within oligosaccharides (22, 23). The correct positioning of the sulfo groups in the NRE oligosaccharides by MS/MS will only leave the determination of the iduronic and glucuronic acid residues to understand the diversity of NRE structures in the heparin polymer.

REFERENCES

1. Davies, J. G., and Henrissat, B. (2002) *Biochem. Soc. Trans.* **30,** 291–297
2. Cataldi, T. R., Campa, C., and de Benedetto, G. E. (2000) *Fresenius' J. Anal. Chem.* **368,** 739–758
3. Koketsu, M., and Linhardt, R. J. (2000) *Anal. Biochem.* **283,** 136–145
4. Packer, N. H., and Harrison, M. J. (1998) *Electrophoresis* **19,** 1872–1882
5. Mulloy, B. (1996) *Mol. Biotechnol.* **6,** 241–265
6. Esko, J. D., and Selleck, S. B. (2002) *Annu. Rev. Biochem.* **71,** 435–471
7. Rabenstein, D. L. (2002) *Nat. Prod. Rep.* **19,** 312–331
8. Linhardt, R. J., and Gunay, N. S. (1999) *Sem. Thromb. Hemost.* **25,** 5–15
9. Linhardt, R. J., and Toida, T. (1997) in *Carbohydrates as Drugs* (Witczak, Z. B., and Nieforth, K. A., eds) pp. 277–341, Marcel Dekker, Inc., New York
10. Hileman, R. E., Fromm, J. R., Weiler, J. M., and Linhardt, R. J. (1998) *BioEssays* **20,** 156–167
11. Capilla, I., and Linhardt, R. J. (2002) *Angew. Chem. Int. Ed. Engl.* **41,** 390–412
12. Rosenberg, R. D., and Lam, L. (1999) *Proc. Natl. Acad. Sci. U. S. A.* **76,** 1218–1222
13. Kinoshita, A., Yamada, S., Haslam, S. M., Morris, H. R., Dell, A., and Sugahara, K. (1997) *J. Biol. Chem.* **272,** 19656–19665
14. Drummond, K. J., Yates, E. A., and Turnbull, J. E. (2001) *Proteomics* **1,** 304–310
15. Imanari, T., Toida, T., Koshiishi, I., and Toyoda, H. (1996) *J. Chromatogr. A* **720,** 275–293
16. Rice, K. G., Kim, Y. S., Grant, A. C., Merchant, Z. M., and Linhardt, R. J. (1985) *Anal. Chem.* **150,** 325–331
17. Pervin, A., Gallo, C., Jandik, K. A., Han, X. J., and Linhardt, R. J. (1995) *Glycobiology* **5,** 83–95
18. Yang, H. O., Gunay, N. S., Toida, T., Kuberan, B., Yu, G. L., Kim, Y. S., and Linhardt, R. J. *Glycobiology* **10,** 1033–1040
19. Juhasz, P., and Biemann, K. (1994) *Proc. Natl. Acad. Sci. U. S. A.* **91,** 4333–4337
20. Chai, W. G., Luo, J. L., Lim, C. K., and Lawson, A. M. (1998) *Anal. Chem.* **70,** 2060–2066
21. Kim, Y. S., Ahn, M. Y., Wu, S. J., Kim, D. H., Toida, T., Teesch, L. M., Park, Y., Yu, G., Lin, J., and Linhardt, R. J. (1988) *Glycobiology* **8,** 869–877
22. Lamb, D. J., Wang, H. M., Mallis, L. M., and Linhardt, R. J. (1992) *J. Am. Soc. Mass Spectrom.* **3,** 797–803
23. Siegel, M. M., Tabei, K., Kagan, M. Z., Vlahov, I. R., Hileman, R. E., and Linhardt, R. J. (1997) *J. Mass Spectrom.* **32,** 760–772
24. Zaia, J., McClellan, J. E., and Costello, C. E. (2001) *Anal. Chem.* **73,** 6030–6039
25. Zaia, J., and Costello, C. E. (2001) *Anal. Chem.* **73,** 233–239
26. Shriver, Z., Raman, R., Venkataraman, G., Drummond, K., Turnbull, J., Toida, T., Linhardt, R. J., Biemann, K., and Sasisekharan, R. (2000) *Proc. Natl. Acad. Sci. U. S. A.* **97,** 10365–10370
27. Mikhailov, D., Linhardt, R. J., and Mayo, K. H. (1997) *Biochem. J.* **328,** 51–61
28. Peter-Katalinic, J. (1994) *Mass Spectrom. Rev.* **13,** 77–98
29. Fura, A., and Leary, J. A. (1993) *Anal. Chem.* **65,** 2805–2811
30. Reinhold, V. N., Reinhold, B. B., and Costello, C. E. (1995) *Anal. Chem.* **67,** 1772–1784
31. Harvey, D. J. (1996) *J. Chromatogr. A* **720,** 429–446
32. Khoo, K. H., Morris, H. R., McDowell, R. A., Dell, A., Maccarana, M., and Lindahl, U. (1993) *Carbohydr. Res.* **244,** 205–223
33. Col, R. D., Silverstro, L., Naggi, A., Torri, G., Baiocchi, C., Moltrasio, D., Cedro, A., and Viano, I. (1993) *J. Chromatogr. A* **647,** 289–300
34. Takagaki, K., Munakata, H., Nakamura, W., Matsuya, H., Majima, M., and Endo, M. (1998) *Glycobiology* **8,** 719–724
35. Monstaudo, G., Montaudo, M. S., Puglisi, C., and Samperi, F. (1995) *Rapid Commun. Mass Spectrom.* **9,** 453–462
36. Jackson, C., Larsen, B., and McEwen, C. (1996) *Anal. Chem.* **68,** 1303–1308
37. Deery, M. J., Stimson, E., and Chappell, C. G. (2001) *Rapid Commun. Mass Spectrom.* **15,** 2273–2283
38. Yeung, B., and Mareeak, D. (1999) *J. Chromatogr. A* **852,** 573–581
39. Venkataraman, G., Shriver, Z., Raman, R., and Sasisekharan, R. (1999) *Science* **286,** 537–542
40. Price, K. N., Tuinman, A., Baker, D. C., Chisena, C., and Cysyk, R. L. (1997) *Carbohydr. Res.* **303,** 303–311
41. Mohsin, S. B. (2000) *J. Chromatogr. A* **884,** 23–30
42. Guan, F., Isii, A., Seno, H., Watanabe-Suzuki, K., Kumazuwa, T., and Suzuki, O. (1999) *J. Chromatogr. B* **731,** 155–165
43. Storm, T., Reemtsma, T., and Jekel, M. (1999) *J. Chromatogr. A* **854,** 175–185
44. Conboy, J. J., Henion, J. D., Martin, M. W., and Zweigenbaum, J. A. (1990) *Anal. Chem.* **62,** 800–807
45. Witters, E., Van Donger, W., Esmans, E. L., and Van Onckelen, H. A. (1997) *J. Chromatogr. B* **694,** 55–63
46. Kuberan, B., Lech, M., Zhang, L., Wu, Z. L., Beeler, D. L., and Rosenberg, R. D. (2002) *J. Am. Chem. Soc.* **124,** 8707–8718
47. Edens, R. E., Al-Hakim, A., Weiler, J. M., Rethwisch, D. G., Fareed, J., and Linhardt, R. J. (1992) *J. Pharm. Sci.* **81,** 823–827
48. Thanawiroon, C., and Linhardt, R. J. (2003) *J. Chromatogr. A,* **1014,** 215–223
49. Cai, J., and Henion, J. D. (1995) *J. Chromatogr. A* **703,** 667–692
50. Huber, C. G., and Krajete, A. (2000) *J. Chromatogr. A* **870,** 413–424
51. Cheng, X., Gale, D. C., Udseth, H. R., and Smith, R. D. (1995) *Anal. Chem.* **67,** 586–593
52. Stephenson, J. L., Jr., and McLuckey, S. A. (1998) *Anal. Chem.* **70,** 3533–3544
53. Griffey, R. H., Sasmor, H., and Grieg, M. J. (1997) *J. Am. Soc. Mass Spectrom.* **8,** 155–160
54. Jandik, K. A., Gu, K., and Linhardt, R. J. (1994) *Glycobiology* **4,** 289–296
55. Rice, K. G. (1997) *A Sequencing Strategy for Heparin.* Doctoral thesis, College of Pharmacy, University of Iowa, Iowa City
56. Linhardt, R. J., Merchant, Z. M., Rice, K. G., Kim, Y. S., Fitzgeald, G. L., Grant, A. C., and Langer, R. (1985) *Biochemistry* **24,** 7805–7810
57. Linhardt, R. J., Cohen, D. M., and Rice, K. G. (1989) *Biochemistry* **28,** 2888–2894
58. Nader, H. B., Porcionatto, M. A., Tersariol, I. L. S., Pinhal, M. A. S., Oliveira, F. W., Moraes, C. T., and Dietrich, C. P. (1990) *J. Biol. Chem.* **265,** 16807–16813
59. Okada, Y., Yamada, S., Toyoshima, M., Dong, J., Nakajima, M., and Sugahara, K. (2002) *J. Biol. Chem.* **277,** 42488–42495
60. Gong, F., Jemth, P., Escobar-Galvis, M. L., Vlodavsky I., Horner, A., Lindahl, U., and Li, J. (2003) *J. Biol. Chem.* **278,** 35152–35158
61. Loganathan, D. Wang, H. M. Mallis, L. M., and Linhardt, R. J. (1990) *Biochemistry,* **29,** 4362–4368
62. Yamada, S., Sakamoto, K., Tsuda, H., Yoshida, K., Sugahara, K., Khoo, K. H., Morris, H. R., and Dell, A. (1994) *Glycobiology* **4,** 69–78
63. Liu, J., Desai, U. R., Han, X. J., Toida, T., and Linhardt, R. J. (1995) *Glycobiology* **5,** 765–774
64. Yamada, S., Sakamoto, K., Tsuda, H., Yoshida, K., Sugiura, M., and Sugahara, K. (1999) *Biochemistry* **38,** 838–847
65. Merry, C. L., Lyon, M., Deakin, J. A., Hopwood, J. J., and Gallagher, J. T. (1999) *J. Biol. Chem.* **274,** 18455–18462
66. Turnbull, J. E., Hopwood, J. J., and Gallagher, J. T. (1999) *Proc. Natl. Acad. Sci. U. S. A.* **96,** 2698–2703
67. Kinoshita, A., and Sugahara, K. (1999) *Anal. Biochem.* **269,** 367–378
68. Midura, R. J., Calabro, A., Yanagishita, M., Hascall, V. C. (1995) *J. Biol. Chem.* **270,** 8009–8015